

Incorporating "sinuous connectivity" into stochastic models of crustal heterogeneity: Examples from the Lewisian gneiss complex, Scotland, the Franciscan formation, California, and the Hafafit gneiss complex, Egypt.

John A. Goff, *Institute for Geophysics, University of Texas*

Alan Levander, *Rice University*

AFOSR Contract F49620-94-1-0100

Abstract. Stochastic models are valuable and sometimes essential tools for investigating the behavior of complex phenomena. In seismology, stochastic models can be used to describe velocity heterogeneities that are too small or too numerous to be described deterministically. Where analytic approaches are often infeasible, synthetic realizations of such models can be used in conjunction with finite difference algorithms to systematically investigate the response of the seismic wavefield to complex heterogeneity. This paper represents a continuing effort at formulating a complete and robust stochastic model of lithologic heterogeneity within the crust, and the means of generating synthetic realizations; "complete" implies that the model is flexible enough to describe all types of random heterogeneity within the crust, while "robust" implies sufficiently constrained parameterization that an inversion problem may be well-posed. We use as a basis for investigation geologic maps of crustal exposures and petrophysically inferred velocities. Earlier efforts at stochastic modeling have focused on characterization of the univariate probability density function, which is typically modal (i.e., binary, ternary, etc.), and the covariance function, which is typically fit with a von Kármán function. Here we provide a means of characterizing the property of "sinuous connectivity" and for generating realizations that possess this property. Sinuous connectivity is the tendency for individual lithologic units to be continuous over long and highly contorted paths; there is no means in the earlier modeling of either characterizing or synthesizing this property. We first demonstrate that binary sinuously connective realizations can be generated by mapping alternating contour sets from a Gaussian-distributed surface (a "normal equivalent field") into the two values comprising the binary probability density. There is tremendous non-uniqueness in this operation, with wide classes of mapping functions and normal equivalent statistics resulting in model fields that are statistically identical. We infer from these observations that the property of sinuous connectivity can be represented by a simple binary yes-or-no parameter.

Keywords: lithospheric heterogeneity, sinuous connectivity, covariance modeling, stochastic models

19960624 160

I. Introduction

Investigations of the wavefield response to heterogeneous media (finite difference or otherwise) can be of a deterministic (i.e., the exact particulars) or stochastic (i.e., ensemble properties) nature. The choice of one or the other is a matter of scale, numbers, and resolution. The deterministic approach is typically used when the structures within the velocity field are few in number and large compared to the seismic wavelength. In such cases a well-posed inverse problem may be formulated to estimate the velocity field by, for example, matching a synthetic wavefield to the observed wavefield [e.g., *Jervis et al.*, 1995]. The stochastic approach is necessary when structures within the velocity field are numerous and/or small compared to the wavelength. Large numbers of scattering features tend to make the wavefield complex (i.e., deterministically unpredictable) through both single and multiple forward and backward scattering. Small scales make deterministic resolution of structures difficult or impossible. Recent studies have used finite difference algorithms to investigate the seismic wavefield response to synthetic realizations of stochastic velocity models [e.g., *Frankel and Clayton*, 1986; *Fisk et al.*, 1992; *Holliger et al.*, 1993; *Levander et al.*, 1994a,b]. So far these efforts have only been directed toward the forward problem, where a velocity model is assumed and the wavefield response computed. Qualitative comparisons of seismic data with finite-difference seismograms generated in a variety of realistic circumstances suggest that the seismogram is sensitive to variations in the stochastic character of the medium. Efforts are now being directed towards establishing quantitatively meaningful model/data comparisons to pose the inverse problem of estimating stochastic properties of a velocity field from observations of the seismic wavefield.

This report is one in a series of efforts to establish a "robust" and "complete" stochastic model for crustal heterogeneity through analysis of mapped crustal exposures. Though modified by the act of exhumation, crustal exposures represent our only direct multidimensional sampling of crustal rocks from depth. They provide invaluable information on lithologies and their spatial relationships. The principal goal of working with this data is not to establish precisely the stochastic nature of the crust, but rather to ascertain the types of stochastic models that are appropriate. By "robust" we intend a model with few-enough parameters that an inversion problem may be well-posed. By "complete" we intend a model that can reproduce, through synthetic realization, all the important physical properties of the field. There is a delicate balance between these two concerns. If we have too few parameters in the desire for robustness, then the model may not be flexible enough to characterize the variety of stochastic morphology observed. If we favor completeness we may require more parameters than we can ever hope to solve for in an inverse problem.

Previous work on mapped crustal exposures has focused on combined modeling of the covariance function and probability density function (PDF) of the velocity field (as inferred from petrophysical conversion of the lithographic field). The covariance function has often been successfully modeled using the *von Kármán* [1948] model [e.g., *Holliger et al.*, 1993; *Levander et al.*, 1994]. The PDF has often been modeled by a simple modal distribution (e.g., binary, ternary, etc.) [*Holliger et al.*, 1993; *Levander et al.*, 1994; *Goff et al.*, 1994], which reflects the observation that mapped crustal exposures, even morphologically complex ones, typically consist of a small number of distinct lithologic units of relatively constant velocity. Synthetic realizations generated from these models successfully reproduce many of the important physical properties of the observed field, including the modal PDF, characteristic scales, structural anisotropy, and fractal dimension. However, one property clearly seen on many of the crustal exposures has thus far remained beyond the grasp of stochastic characterization: "sinuous connectivity", the subject of this report.

Sinuous connectivity is a difficult property to define in words, but simple to demonstrate. Figure 1a is a digitized section of the Lewisian gneissic terrain (Scotland), an exposed section of the middle crust consisting primarily of amphibolite dikes (black) and gneiss (white) (gray = no data). The gneiss has a petrophysically inferred p-wave velocity of 6.2 km/sec, and the amphibolite 6.75 km/sec. *Levander et al.*, [1994a] formulated a stochastic model based on analysis of the PDF and covariance structure for the grid shown in Figure 1, and a synthetic realization from a refined version of this model is presented in Figure 1b. The grids shown in Figures 1a and 1b have essentially identical PDF and covariance, and those physical attributes characterized by those functions are well-matched; i.e., the percentage of gneiss and amphibolite, the characteristic scales, and the fractal dimension (the overall degree of roughness). Nevertheless the comparison is not satisfactory. The amphibolite in the geologic map is highly connected and sinuous, whereas in the synthetic field it is disconnected and blob-like.

In this paper we present a method for incorporating sinuous connectivity into stochastic models for lithologic (i.e., modal) heterogeneity, and the means by which to generate a sinuously connective synthetic realization that honors the covariance and PDF structure specified by the stochastic model. The success of this approach is demonstrated in Figure 1c, which displays a sinuously connective synthetic field with identical PDF and covariance structure to the synthetic shown in Figure 1b. The comparison between this synthetic to the Lewisian data in Figure 1a is clearly superior; we believe that this stochastic model, incorporating PDF (modal or otherwise), covariance, and sinuous connectivity characterization, represents as complete a model as might be necessary for characterizing seismic velocity heterogeneity within the earth. The robustness of this model, as applied to seismic inversion, will be the topic of future investigation.

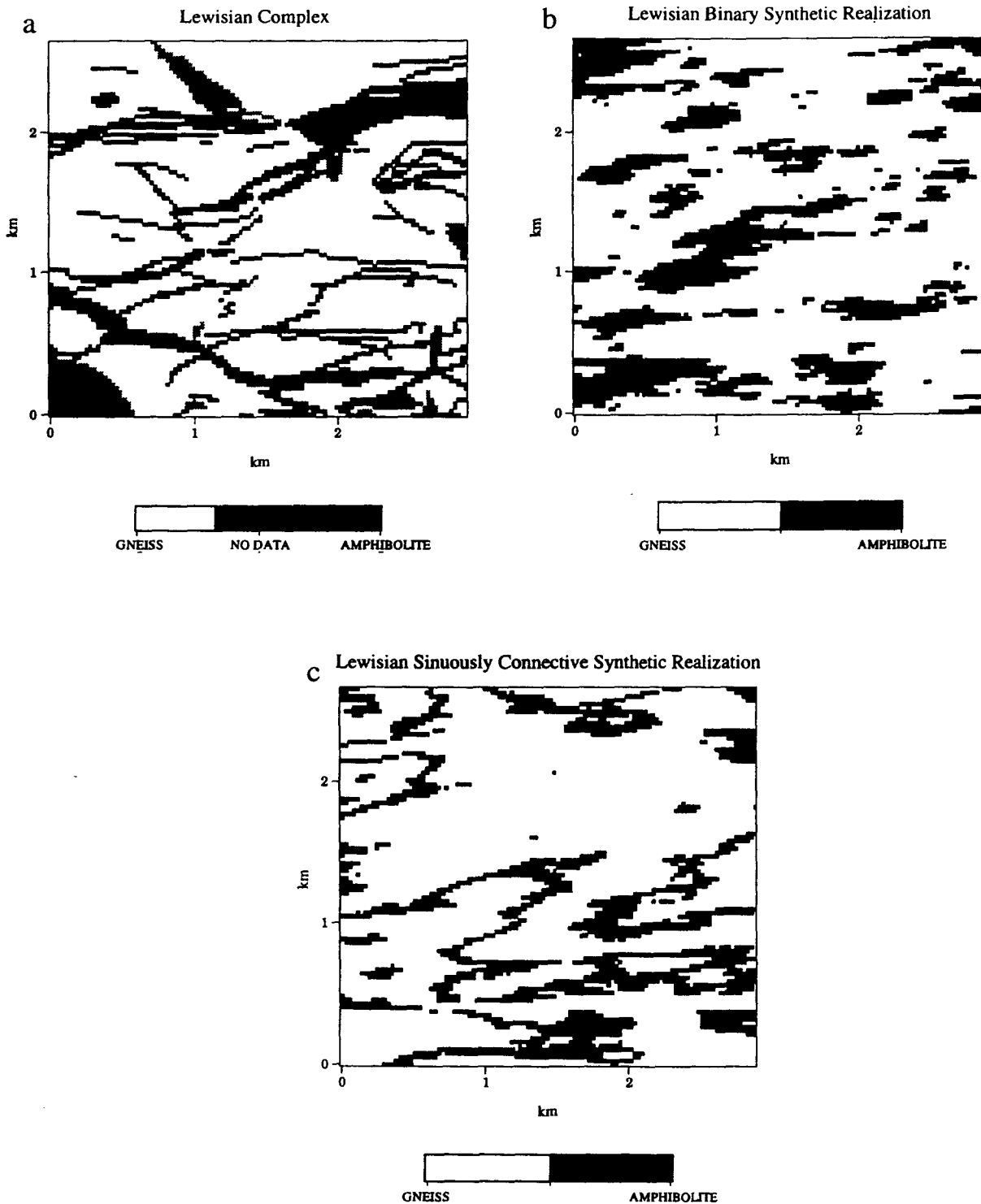


Figure 1. (a) Digitized map of the Lewisian gneiss complex, Scotland [Levander *et al.*, 1994]. Also mapped but not shown are intermediate schist, which comprise only 1% of the total and so were ignored as insubstantial. Map is 78% gneiss (6200 m/sec inferred p-wave velocity) and 22% amphibolite (6750 m/sec). The grid spacing is 0.0268 km, with 100 rows and 109 columns. (b) Synthetic realization based on PDF and covariance modeling of the Lewisian complex. (c) Synthetic realization based on PDF and covariance modeling of the Lewisian complex and including the property of sinuous connectivity.

II. PDF and Covariance Modeling and Synthetics

Details regarding PDF and covariance modeling based on crustal exposure maps are given in *Holliger et al.* [1993] and *Levander et al.* [1994a]. Heretofore covariance modeling has been accomplished by forward-model fitting of the von Kármán function to the data covariance. Here we apply the inversion algorithm of *Goff and Jordan* [1988] converted to use with gridded data. The method for generating synthetic realizations from such models is given in *Goff et al.* [1994]. In this section we provide a brief overview of the salient points from these references.

PDF Modeling

In the case of a modal field, modeling the PDF is robust and straightforward: the PDF simply describes the percentage of each unit present in the field. For example, in the Lewisian section described above, 78% of the map is gneiss, and the remaining 22% is amphibolite (Figure 2a).

Covariance Modeling

The covariance function, or its Fourier equivalent the power spectrum, represents our primary tool for characterizing spatial roughness properties. It is defined by:

$$C_{hh}(\mathbf{x}) = E[h(\mathbf{x}_1)h(\mathbf{x}_1 + \mathbf{x})], \quad (1)$$

where $h(\mathbf{x}_1)$ is a zero-mean, homogeneous random field specified at vector location \mathbf{x}_1 , and $E[\bullet]$ represents the expectation function [e.g., *Feller*, 1971]. The variable \mathbf{x} is defined as the lag vector. Where h is sampled on a m by n grid specified by discrete (column,row) locations (i,j) , the discrete covariance function $C_{hh}(k,l)$ can be estimated by

$$\bar{C}_{hh}(k,l) = \frac{1}{(n-k)(m-l)} \sum_{i=1}^{n-k} \sum_{j=1}^{m-l} h_{i,j} h_{i+k,j+l}. \quad (2)$$

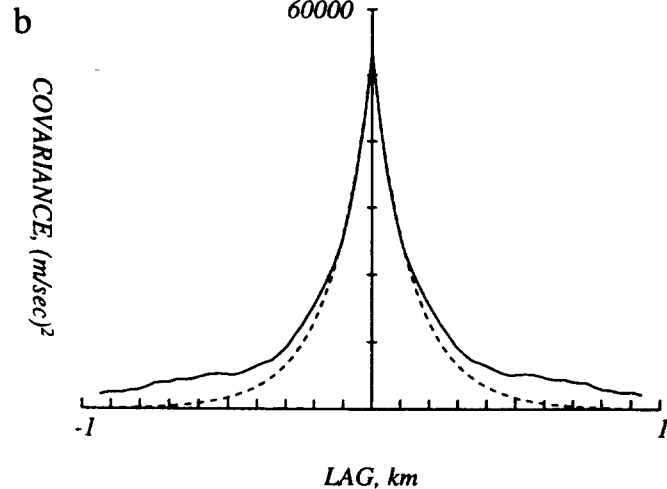
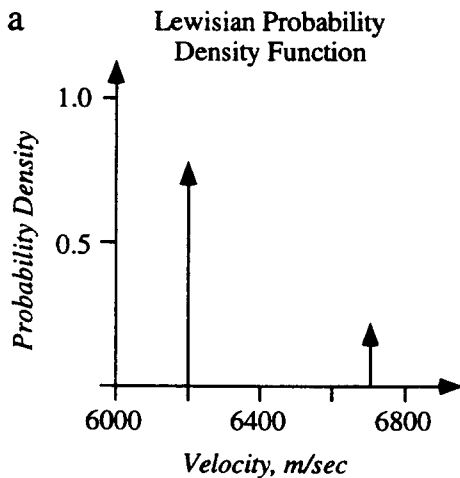


Figure 2. (a) PDF for the Lewisian stochastic model. (b) Comparison of Lewisian data (solid) and best-fit model (dashed) 1-D covariances for the row direction ($C_{hh}(i,0)$).

Covariance modeling is typically accomplished by fitting a parameterized functional model to the sample covariance estimated from the digital exposure map using forward modeling [e.g., *Holliger et al.*, 1993; *Levander et al.*, 1994a; *Holliger and Levander*, 1994] or a least-squares inversion [*Goff and Jordan*, 1988]. The von Kármán [1948] covariance model [e.g., *Wu and Aki*, 1985; *Frankel and Clayton*, 1986; *Fisk et al.*, 1992; *Holliger et al.*, 1993; *Levander et al.*, 1994a, *Holliger and Levander*, 1994] represents a class of monotonically decaying (i.e., aperiodic) functions, and includes as a subset the exponential form. The singular advantage of the von Kármán model is that it explicitly includes the fractal dimension as a variable. *Goff and Jordan* [1988] modified the von Kármán covariance function to account for structural anisotropy in 2-dimensions (easily expanded to 3-dimensions). The following parameters specify the 2-D anisotropic von Kármán model:

1. The rms velocity H is the average variation about the mean velocity.

2. The lineament orientation θ_s is strike of direction of maximum correlation; structures will tend to be oriented along this direction.

3. The scale parameter controls the rate of decay of the covariance. In one dimension the scale parameter is specified by k_0 . In two dimensions there are two principal scale parameters: k_n in the normal-to-strike direction, and k_s in the along-strike direction; $k_n > k_s$.

4. The aspect ratio a is the characteristic planar shape of structures, defined by the ratio k_n/k_s .

5. The Hausdorff (fractal) dimension D is a measure of roughness.

An inversion procedure for parameter estimation also provides estimates of uncertainties. Estimated Lewisian model parameters are, with 1- σ uncertainties: $H = 234 \pm 4$ m/sec, $\theta_s = 85.0^\circ \pm 0.4^\circ$, $k_n = 24.5 \pm 1.0$ km $^{-1}$, $k_s = 6.0 \pm 0.3$ km $^{-1}$, and $D = 2.54 \pm 0.04$. Figure 2b displays the best fit von Kármán model to the 1-D sample covariance in the row direction ($C_{hh}(i,0)$).

Synthetic Fields

Realizations of the stochastic model described above can be synthesized by first generating a Gaussian-distributed field, which we term a "normal equivalent" field, and then mapping it into a new field, the "model" field, that conforms to the PDF specified in the model. This algorithm includes the following steps [Goff et al., 1994]:

1. A mapping function is created which specifies the conversion of a Gaussian PDF with zero mean and unit variance to the PDF $p(h)$ specified by the stochastic model. Specifically, for each possible value g sampled from a Gaussian PDF $p_G(g)$, we find a new value h such that:

$$\int_{-\infty}^h p(h') dh' = \int_{-\infty}^g p_G(g') dg'. \quad (3)$$

For a simple binary field, where unit 1 has total probability ρ_1 , and unit 2 has total probability $\rho_2 = 1 - \rho_1$, equation (3) is equivalent to identifying a cutoff Gaussian value g_c , where every value less than g_c is mapped to unit 1, and every value greater than g_c is mapped to unit 2, and

$$\rho_1 = \int_{-\infty}^{g_c} p_G(g') dg'. \quad (4)$$

For the Lewisian PDF, $g_c = 0.75$. Hence, for the Lewisian model field, any Gaussian value less than 0.75 is mapped to gneiss, and everything else to amphibolite.

2. The covariance for the normal equivalent field, $C_{gg}(x)$, is determined such that when the PDF mapping described above is performed, the model field conforms to the model covariance $C_{hh}(x)$. Where both normal equivalent and model fields have zero mean and unit variance, the relationship is given by Christakos [1992; page 332, equation 3]. In general this equation must be solved by numerical integration.

3. Generate a synthetic normal equivalent realization $g(i,j)$ conforming to covariance $C_{gg}(k,l)$ by Fourier methods [e.g., Goff and Jordan, 1988; 1989a].

4. For each discrete value of the normal equivalent $g(i,j)$, determine the value of the model field $h(i,j)$ using the PDF mapping described in step 1.

The Lewisian Data/Synthetic Comparison, Take 1

The Lewisian 2-D stochastic model is summarized as follows: (1) The PDF is a binary distribution of 78% gneiss (6.2 km/s) and 22% amphibolite (6.75 km/s); (2) the covariance is modeled by a von Kármán function specified by parameters $k_n = 24.5 \text{ km}^{-1}$, $k_s = 6.0 \text{ km}^{-1}$, $\theta_s = 85.0^\circ$ (where 0° represents vertical lineament orientation), and $D = 2.54$. Figure 1b displays a full two-dimensional synthetic realization of the stochastic model estimated from the

Lewisian map of Figure 1a. The covariance parameters for the normal equivalent field are: $k_n = 21.6 \text{ km}^{-1}$, $k_s = 5.28 \text{ km}^{-1}$, $\theta_s = 85.0^\circ$, and $D = 2.00$.

As stated in the Introduction, comparison between Figures 1b, the synthetic realization of the stochastic model, and Figure 1a, the data from which the stochastic model is derived, indicates both successes and failures of the stochastic model. The success of the model is that it correctly describes the physical properties that it is designed to describe; i.e., probability of units, scales of structures, orientation, and roughness. The failure of the model is that it is not complete; i.e., it cannot reproduce the pattern which is visually obvious to the eye: the sinuous connectivity of the units.

III. Sinuous Connectivity Modeling and Synthetics

Till now we have employed a stochastic modeling technique which requires joint characterization of the PDF and covariance of the field of interest. A great advantage of this technique is that estimation of model parameters can be performed through direct inversion of sample data. An entirely equivalent, though indirect, stochastic modeling technique would be joint specification of a PDF mapping and the covariance function of a normal equivalent: i.e., the "recipe" for generating synthetic realizations. In the case of the Lewisian model discussed above, this type of stochastic model would be specified by the normal equivalent covariance parameters $k_n = 21.6 \text{ km}^{-1}$, $k_s = 5.28 \text{ km}^{-1}$, $\theta_s = 85.0^\circ$, and $D = 2.00$, and the Gaussian-to-binary PDF mapping function with separation scale $g_c = 0.75$.

The rationale for adopting the latter approach to stochastic modeling is that it provides an added dimension to characterization not available in the former: the PDF mapping. The PDF mapping presented earlier is, in fact, only the simplest possible case of a Gaussian-to-binary mapping. The only real constraint that is placed on this mapping is that the total probability of unit 1 (gneiss) is 0.78, and the total probability of unit 2 (amphibolite) is 0.22. Instead of finding a single value g_c which separates the Gaussian PDF into regions of 0.78 and 0.22 probability, we can formulate a more complex mapping into alternating bands of unit 1 and unit 2, ensuring that the sum of all unit 1 probability is 0.78, and the sum of all unit 2 probability is 0.22. This operation will map the alternating units onto contour sets of the normal equivalent surface; we therefore apply the term "contour set mapping" to this type of PDF mapping. As anyone who has seen a contour map of topography will quickly intuit, contour set mapping should generate a binary surface possessing the property of sinuous connectivity.

Contour Set Mapping Synthetics

More formally, we specify a binary contour set mapping in the following way:

$$h(\mathbf{x}_1) = \left\{ \begin{array}{ll} H_2, & g_3 < g(\mathbf{x}_1) < g_4 \\ H_1, & g_2 < g(\mathbf{x}_1) < g_3 \\ H_2, & g_1 < g(\mathbf{x}_1) < g_2 \\ H_1, & g_0 = -\infty < g(\mathbf{x}_1) < g_1 \end{array} \right\}, \quad (5)$$

where H_1 and H_2 represent the values given to units 1 and 2 respectively. Each interval defined by the boundary values g_{i-1} to g_i is defined as a "contour set", and the difference $g_i - g_{i-1}$ is defined as the "contour set thickness". Total probabilities for each unit are computed by the following:

$$\rho_1 = \sum_{i \text{ odd}} \int_{g_{i-1}}^{g_i} p_G(g') dg', \quad (6)$$

$$\rho_2 = 1 - \rho_1 = \sum_{i \text{ even}} \int_{g_{i-1}}^{g_i} p_G(g') dg'$$

The boundary values g_i must be chosen so that ρ_1 and ρ_2 satisfy our total probability constraints (for the Lewisian case, ρ_1 must equal 0.78 and ρ_2 must equal 0.22). Beyond that, however, the values of g_i are arbitrary, unfortunately resulting potentially in an infinite number of additional parameters to the model. Limitations on parameters will be discussed below.

While contour set mapping must satisfy total probability constraints, the covariance of the normal equivalent field must be chosen so that the model field corresponds to the model covariance. While we cannot at this time make formal statements of uniqueness, it is nevertheless clear from our experience in forward modeling that, for a given PDF mapping, this is a strong constraint.

Before presenting examples of synthetic realizations generated with contour set mappings, we must remark that von Kármán normal equivalent covariances do not strictly imply von Kármán model covariances, as was the case for simple Gaussian-to-binary mappings [Goff *et al.*, 1994]. This is particularly true where contour sets for either unit 1 or unit 2 or both are not of uniform thickness. Where unit 1 thickness are uniform and unit 2 thicknesses are uniform, the model covariance resulting from a von Kármán normal equivalent covariance can be reasonably approximated by a von Kármán function. The correspondence between the model covariance and a best-fitting von Kármán function in these cases is not always exact, but misfit, where it occurs, is concentrated at the larger lags where resolution of the covariance estimated from data is very poor (i.e., either will fit the data just as well). However, in some cases, two of which will be highlighted in the following section, the covariance estimated from the data field is not well-fit by the von Kármán function;

instead of a simple decay with increasing lag, the covariance of these fields exhibits two scales of decay. The flexibility allowed in the contour set mapping is instrumental in reproducing these more complicated covariance structures.

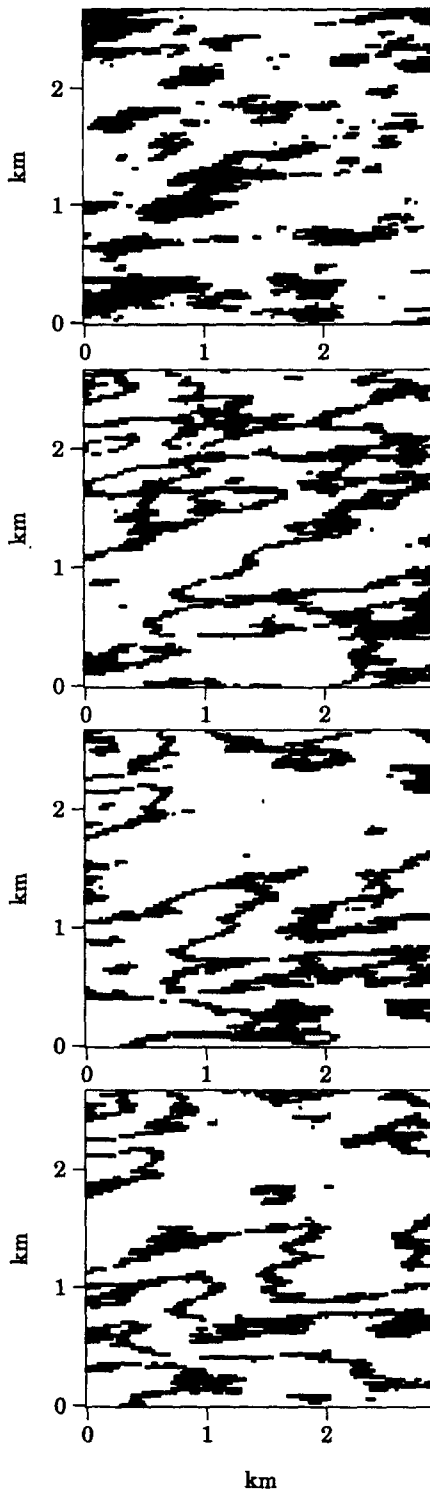
Figure 3 displays a series of four model fields generated using progressively thinner contour sets, labeled as model fields 1-4. The contour set mappings are also shown, displayed graphically as black and white areas below the Gaussian PDF. Each model field PDF and covariance correspond to the stochastic model described earlier for the Lewisian map (Figure 1a). Model field 1 is just a simple Gaussian-to-binary mapping presented earlier as Figure 1b. All the normal equivalent fields were generated with identical random phase spectra, which enhances visual recognition of structural similarities.

Our primary observation derived from Figure 3 is that contour set mappings successfully produce sinuous connectivity in the model field. In particular, model field 3 is identical to the synthetic realization in Figure 1c, which was compared to the data field (Figure 1a) in the Introduction. As noted earlier, this comparison is visually superior to the comparison of Figure 1b (simple Gaussian-to-binary mapping) to Figure 1a.

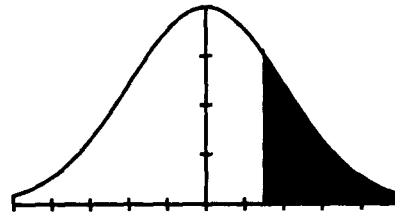
The Sinuous Connectivity Parameter

Now that we've established a method for characterizing and synthesizing fields that possess the property of sinuous connectivity, we ask ourselves if it is possible to quantify sinuous connectivity itself. In other words, might it be possible to state that one field has more or less sinuous connectivity than another field? By stepping through progressively thinner contour set thicknesses, Figure 8 was designed to address this question. If sinuous connectivity were a quantifiable property, then we would expect a general increase in this property as we decrease in contour set thickness in the PDF mapping. However, this does not appear to be the case. While there is a strong contrast in character going from the model field 1 to model field 2 in Figure 3, beyond that there is little noticeable change in character with decreasing contour set thickness. The apparent invariance of sinuous connectivity characteristics is likely attributable to the self-similarity property of the fractal normal equivalent fields [e.g., Mandelbrot, 1981].

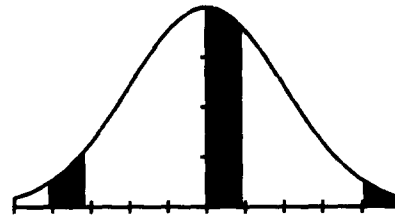
The important implication of the above observation is that wide classes of stochastic models based on contour set mappings and normal equivalent covariances are redundant, or non-unique. On the one hand this is problematic, since it implies that this technique for stochastic modeling will not be useful in an inversion problem. On the other hand, this observation is very powerful, because it vastly simplifies the parameterization that is necessary: the stochastic model is complete just by specifying its PDF, covariance, and whether or not it is sinuously connective.



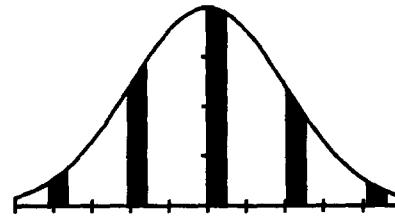
Model Field 1
 Normal Equivalent Parameters:
 $k_n = 21.6 \text{ km}^{-1}$, $k_s = 5.28 \text{ km}^{-1}$, $D = 2.00$



Model Field 2
 Normal Equivalent Parameters:
 $k_n = 4.90 \text{ km}^{-1}$, $k_s = 1.20 \text{ km}^{-1}$, $D = 2.04$



Model Field 3
 Normal Equivalent Parameters:
 $k_n = 1.89 \text{ km}^{-1}$, $k_s = 0.46 \text{ km}^{-1}$, $D = 2.10$



Model Field 4
 Normal Equivalent Parameters:
 $k_n = 0.82 \text{ km}^{-1}$, $k_s = 0.20 \text{ km}^{-1}$, $D = 2.10$

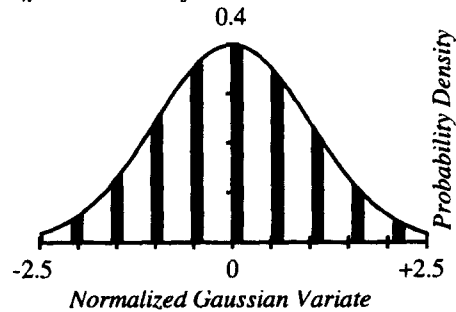


Figure 3. A series of 4 model fields, all with identical PDF and covariance (the Lewisian stochastic model), generated with contour set mappings of decreasing contour set thickness. To the right of each model field, normal equivalent covariance parameters are. All normal equivalent fields had identical H (1.0) and θ_s (85°). Also shown are to the right are graphical representations of the contour set mapping; any value sampled from the normal equivalent field that fell within the white regions was mapped to unit 1, and any sample that fell within the black regions was mapped to unit 2. In Model fields 2 through 4, the contour set thickness changes by a factor of 2 at each step. Model fields 1 and 3 are identical to model field presented in Figures 1a and 1b respectively.

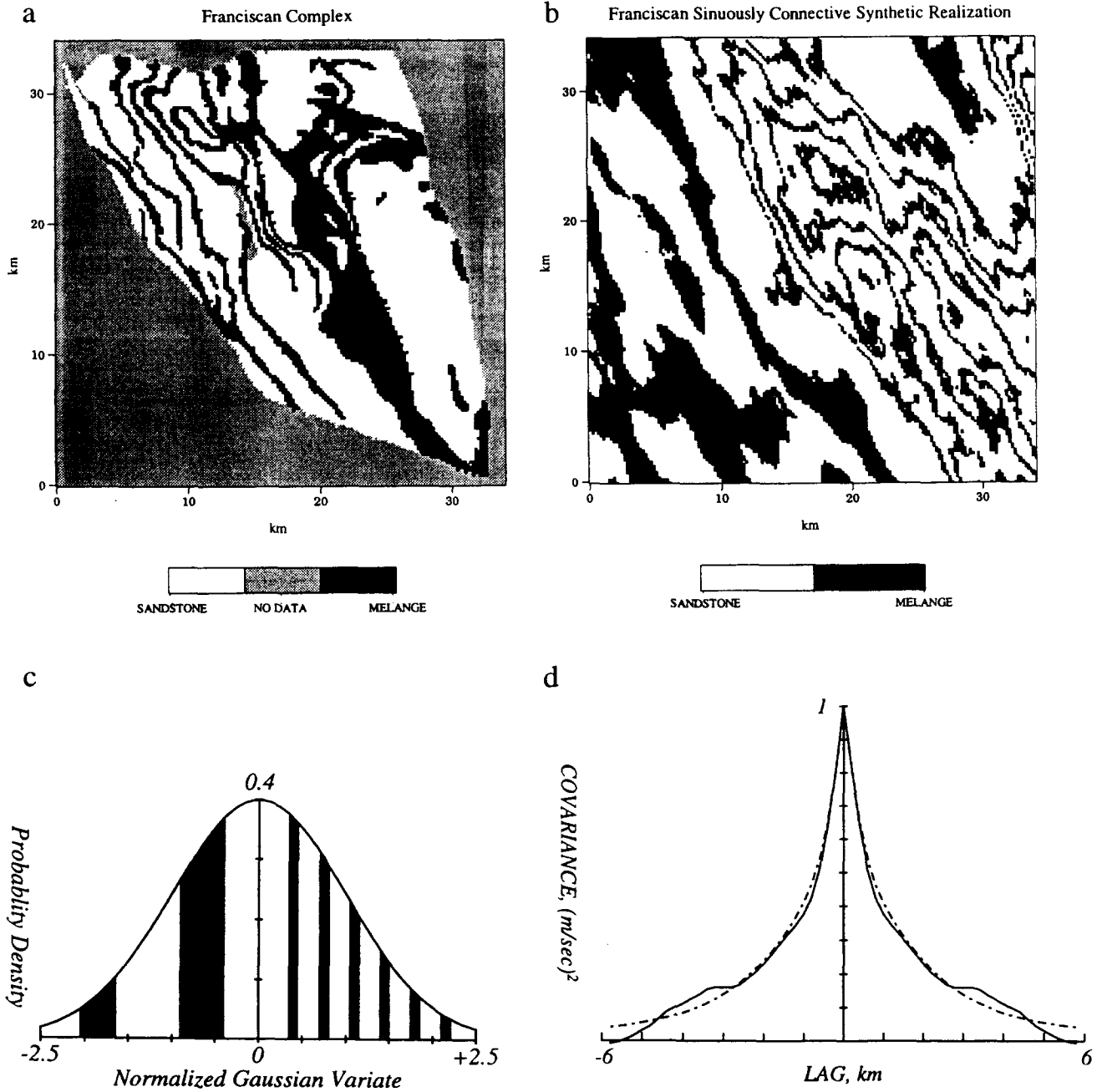


Figure 4. (a) Digitized map of the Franciscan complex, northern California (B.M. Page, 1994, unpublished). A small percentage of volcanic units within the map were ignored as insubstantial. Map is 66% sandstone and 34% melange. While sandstone will have a nearly uniform seismic velocity of ~ 5.8 - 5.9 km/s, melange is expected to exhibit a range of velocities from ~ 5.0 - 6.4 km/s. There are two problems in stochastic modeling associated with the Franciscan: the interaction between melange and sandstone, and the properties of the melange. For the present we concentrate on the former, and simply identify sandstone and melange with proxy values -1 and $+1$. (b) Synthetic realization based on PDF and covariance modeling of the Franciscan complex, including 2-scaled contour set mapping and the property of sinuous connectivity. Normal equivalent parameters are listed in text. (c) Graphical representation of the Franciscan contour set mapping; any value sampled from the normal equivalent field that fell within the white regions was mapped to unit 1 (sandstone), and any sample that fell within the black regions was mapped to unit 2 (melange). (d) Comparison of the Franciscan 1-D column-direction ($C_{hh}(0,j)$) data covariance (solid) with the model covariance (dashed) computed for the 2-scaled, sinuously connective field.

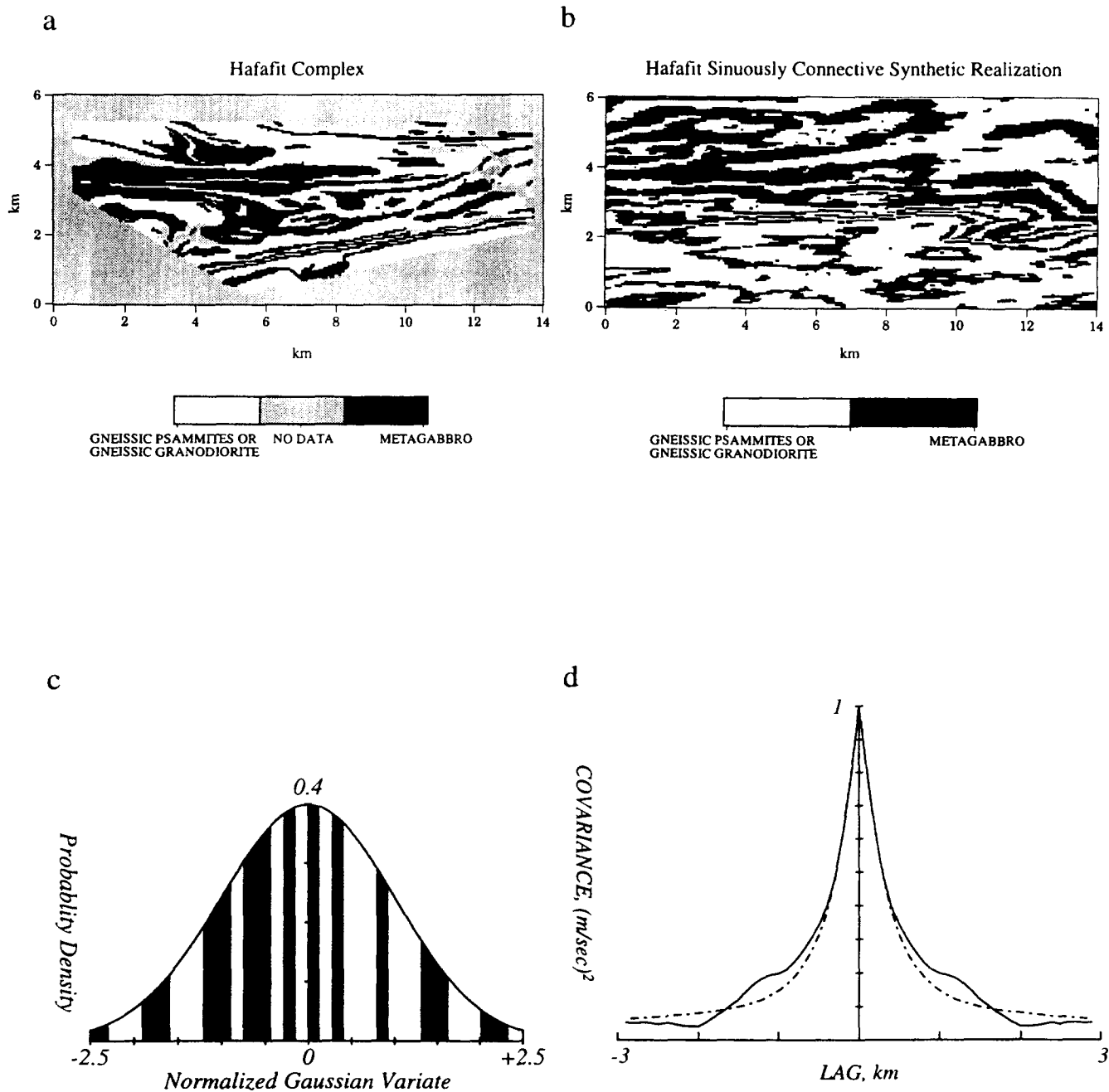


Figure 5. (a) Digitized map of the Hafafit complex, eastern Egypt [Greiling and El-Ramly, 1990; Rashwan, 1991]. The gneissic psammites and gneissic granodiorites have only incidental contact, and so were considered as one unit to increase coverage. A small percentage of granites were ignored as insubstantial. Where it was clearly obvious to do so, units were interpolated where covered by wadi alluvium. Map contains 50% gneiss and 50% metagabbro. Petrophysical data are not known, so proxy values of -1 and +1 were assigned respectively to the gneiss and metagabbro. It is certain, however, that the metagabbro will have a faster seismic velocity than the gneiss. (b) Synthetic realization based on PDF and covariance modeling of the Hafafit complex, including 2-scaled contour set mapping and the property of sinuous connectivity. Normal equivalent parameters are listed in text. (c) Graphical representation of the Hafafit contour set mapping; any value sampled from the normal equivalent field that fell within the white regions was mapped to unit 1 (gneiss), and any sample that fell within the black regions was mapped to unit 2 (metagabbro). (d) Comparison of the Hafafit 1-D row-direction ($C_{hh}(i,0)$) data covariance (solid) with the model covariance (dashed) computed for the 2-scaled, sinuously connective field.

IV. Complex Examples

Two more examples of sinuous connectivity modeling are presented in Figures 4 (Franciscan formation) and 5 (Hafafit gneiss complex). These examples are more complex than the Lewisian example because their covariance functions were not well-fit by a von Kármán model. In particular, we required two superposed scales of decay. This behavior can be matched, however, in the contour set mapping not by formulating a complex normal equivalent field, but rather by using complex combinations of contour thicknesses. Normal equivalent field parameters for the Franciscan are: $k_N = 0.144 \text{ km}^{-1}$, $k_S = 0.052 \text{ km}^{-1}$, $\theta_S = -26.3^\circ$, and $D = 2.00$. Normal equivalent field parameters for the Hafafit are: $k_N = 0.43 \text{ km}^{-1}$, $k_S = 0.080 \text{ km}^{-1}$, $\theta_S = 91.1^\circ$, and $D = 2.10$.

V. Conclusions

Previous work in stochastic modeling of lithologic heterogeneity has involved joint characterization of the PDF, which is usually modal (i.e., binary, ternary, etc.), and the covariance function, which is often well-represented by the von Kármán function. In this paper we have built upon that earlier work by incorporating, in addition to PDF and covariance characterization, a method for modeling fields that possess the property of sinuous connectivity. This method involves defining a Gaussian-to-binary contour set mapping and a normal equivalent field such that, when the normal equivalent field is mapped to the binary model field, the PDF and covariance of the model field honor the stochastic model. This modeling scheme also constitutes a recipe for generating sinuously connective synthetic realizations of the stochastic model.

An important observation derived from synthetic realizations is that, owing to the self similarity property of the fractal normal equivalent fields, sinuous connectivity modeling is highly non-unique. Wide classes of contour set mappings/normal equivalent fields will generate statistically identical model fields. It is suggested, therefore, that the property sinuous connectivity can be characterized by a binary parameter: either the field is sinuously connective or it is not.

Stochastic models and synthetic realizations of lithologic heterogeneity should play a critical role in modeling seismic wave propagation through a complex crust. The stochastic model presented here is the most realistic and complete representation of lithologic heterogeneity presented to date. We believe that this model is, in fact, sufficiently "complete" for application to the seismic problem; i.e., additional complexity or parameterization will probably not significantly affect the observed seismic wavefield. Our future plans center around investigating the response of the observed wavefield to parameters of the stochastic model.

References

Christakos, G., *Random field models in Earth sciences*, 474 pp., Academic Press, San Diego, 1992.

- El-Ramly, M. F., and R. O. Greiling, *Wadi Hafafit Area*, 1988.
- Feller, W., *An Introduction to Probability Theory and Its Applications*, vol. 2, 669 pp., John Wiley, New York, 1971.
- Fisk, M. D., E. E. Charrette, and G. D. McCartor, A comparison of phase screen and finite difference calculations for elastic waves in random media, *J. Geophys. Res.*, 97, 12,409-12,423, 1992.
- Frankel, A., and R.W. Clayton, Finite difference simulations of seismic scattering: Implications for the propagation of short-period seismic waves in the crust and models of crustal heterogeneity, *J. Geophys. Res.*, 91, 6465-6489, 1986.
- Goff, J. A., and T.H. Jordan, Stochastic modeling of seafloor morphology: Inversion of Sea Beam data for second-order statistics, *J. Geophys. Res.*, 93, 13,589-13,608, 1988.
- Goff, J. A., K. Holliger, and A. Levander, Modal fields: A new method for characterization of random seismic velocity heterogeneity, *Geophys. Res. Lett.*, 21, 493-496, 1994.
- Greiling, R.O., and M.F. El-Ramy, *Wadi Hafafit Area - Structural Geology*, Geologic map, German Ministry of Research and Technology, Technische Fachhochschule Berlin, Germany, 1990.
- Holliger, K., A. Levander, and J. A. Goff, Stochastic modeling of the reflective lower crust: petrophysical and geological evidence from the Ivrea Zone (Northern Italy), *J. Geophys. Res.*, 98, 11,967-11,980, 1993.
- Holliger, K., and A. Levander, Seismic structure of gneissic/granitic upper crust: geological and petrophysical evidence from the Strona-Ceneri zone (northern Italy) and implications for crustal seismic exploration, *Geophysical Journal International*, 119, 497-510, 1994.
- Jervis, M., M. K. Sen, and P. L. Stoffa, Optimization methods in 2D migration velocity estimation, *Geophysics*, in press, 1995.
- Levander, A., R.W. England, S.K. Smith, R.W. Hobbs, J.A. Goff, and K. Holliger, Stochastic characterization and seismic response of upper and middle crustal rocks based on the Lewisian gneiss complex, Scotland, *Geophys. J. Int.*, 119, 243-259, 1994a.
- Levander, A., S.K. Smith, R.W. Hobbs, R.W. England, D.B. Snyder, and K. Holliger, The Crust as a Heterogeneous "Optical" Medium, or "Crocodiles in the Mist", *Tectonophysics*, 232, 281-297, 1994b.
- Mandelbrot, B. B., *The Fractal Geometry of Nature*, 468 pp., W. H. Freeman, New York, 1983.
- Rashwan, A.A., *Petrography, geochemistry and Petrogenesis of the Migif-Hafafit Gneisses at Hafafit Mine Area, Egypt*, Scientific Series of the International Bureau, 5, Forschungszentrum Julich GmbH, Germany, 1991.
- von Kármán, T., Progress in the statistical theory of turbulence, *J. Mar. Res.*, 7, 252-264, 1948.
- Wu, R.-S., and K. Aki, The fractal nature of the inhomogeneities in the lithosphere evidenced from seismic wave scattering, *Pure Appl. Geophys.*, 123, 805-818, 1985.